C.E. SACLAY
DSM

SERVICE D'ASTROPHYSIQUE

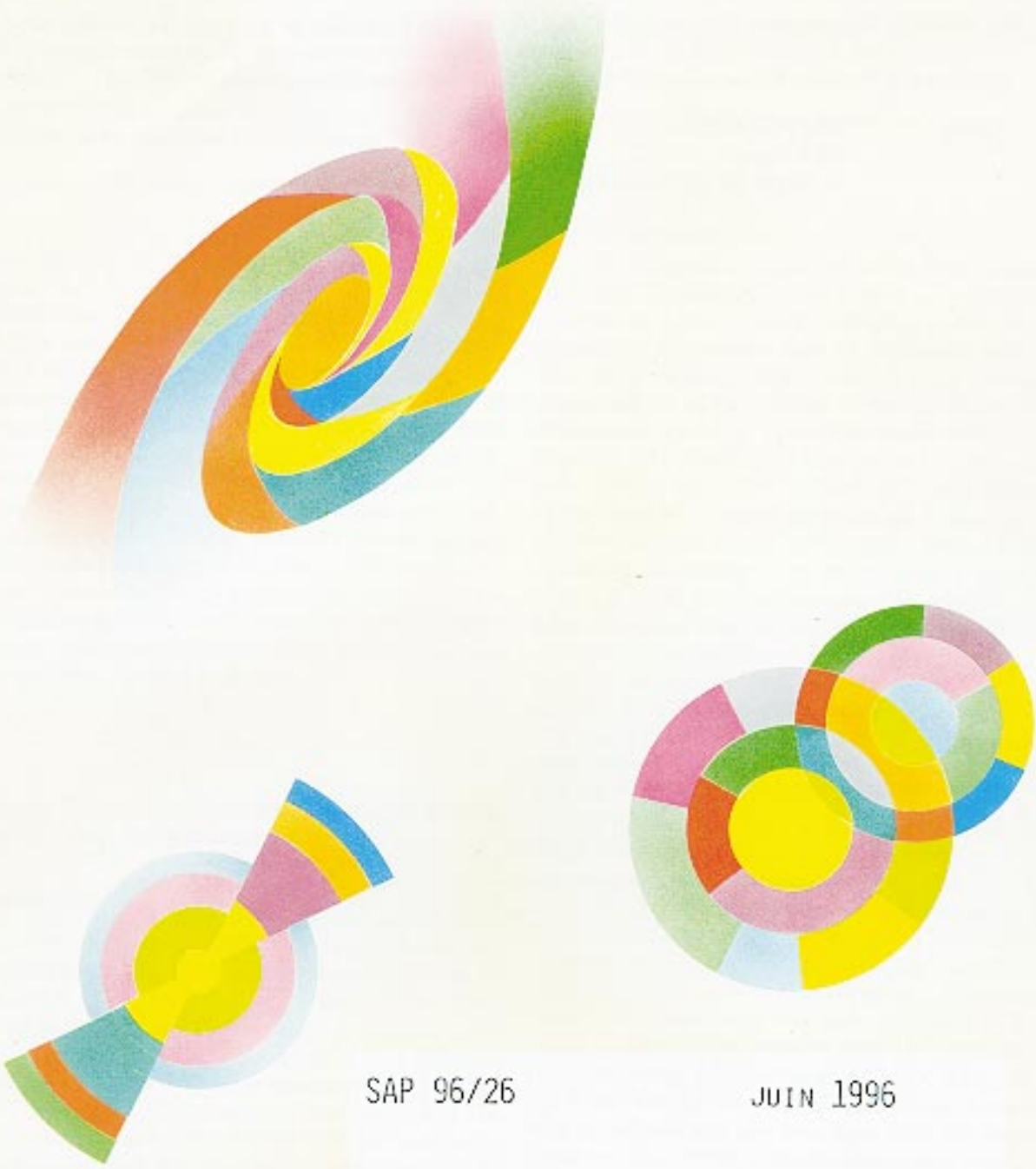

SAP 96/26

JUIN 1996

DISCOVERY OF A JET EMANATING FROM THE PROTOSTAR HH24MMS

DAPNIA

S.BONTEMPS, D.WARD-THOMPSON, P.ANDRE

Le DAPNIA (**D**épartement d'**A**strophysique, de physique des **P**articules, de physique **N**ucléaire et de l'**I**nstrumentation **A**ssociée) regroupe les activités du Service d'Astrophysique (SAp), du Département de Physique des Particules Elémentaires (DPhPE) et du Département de Physique Nucléaire (DPhN).

Adresse : DAPNIA, Bâtiment 141
CEA Saclay
F - 91191 Gif-sur-Yvette Cedex

A&A manuscript no.
(will be inserted by hand later)

Your thesaurus codes are:
06 (08.06.2, 09.09.1 HH24 MMS, 09.10.1)

ASTRONOMY
AND
ASTROPHYSICS
10.7.1996

Discovery of a jet emanating from the protostar HH24 MMS

S. Bontemps[1], D. Ward-Thompson[2], and P. André[1]

[1] CEA/DSM/DAPNIA, Service d'Astrophysique, C.E. Saclay, F-91191 Gif-sur-Yvette Cedex, France
[2] Royal Observatory, Blackford Hill, Edinburgh EH9 3HJ, UK

Received January 17, 1996; Accepted April 5, 1996

Abstract. We report the results of new near-IR, radio continuum, and CO(3–2) observations of the immediate surroundings of the strong submillimetre dust source HH24 MMS. Our near-IR imaging reveals that a short jet of shocked molecular hydrogen is closely associated with the submm clump. The new 3.6 cm map shows that at least part of the radio emission is extended, on a scale consistent with the spatial extension of the near-IR jet. We interpret this elongated centimetre emission as free-free radiation from the shock-ionized portion of the jet. Although our CO(3–2) data do not have enough angular resolution to resolve a bipolar outflow in this complex region, they demonstrate that high-velocity molecular gas is associated with HH24 MMS. Altogether, these results support our earlier claim that the HH24 MMS clump contains a very young Class 0 protostar.

Key words: Stars: formation - ISM: individual objects: HH24 MMS - ISM: jets and outflows

1. Introduction

A prime candidate protostar was recently discovered and labelled HH24 MMS in the Orion B molecular cloud at a distance d $\approx$ 460 pc (Chini et al. 1993). HH24 MMS is a strong source of submillimetre dust continuum emission lying close to the HH24 complex of jets (Mundt, Ray & Raga 1991 and references therein), to the south of SSV63, one of the bright near-infrared sources of the region (Strom, Strom & Vrba 1976). The submm clump is not coincident with any previously known near-IR or optical source. Similarly, no IRAS source is found at this position, and only upper limits can be placed on its IRAS flux densities. HH24 MMS was then initially interpreted as a gravitationally unstable cloud fragment, and hypothesised to be an isothermal protostar with no central hydrostatic core (Chini et al. 1993).

Send offprint requests to: bonte@ariane.saclay.cea.fr

Two subsequent studies of HH24 MMS were carried out, which together suggested it to be an embedded 'Class 0' protostar (André, Ward-Thompson & Barsony 1993 – hereafter AWB) rather than an isothermal protostar. A VLA study of HH24 MMS detected a 3.6 cm radio continuum source at the position of the submillimetre source (Bontemps, André & Ward-Thompson 1995 – hereafter Paper I). The presence of this compact radio source suggests that an embedded, hydrostatic young stellar object (YSO) such as a Class 0 protostar has formed at the centre of the submm clump. At the same time, a JCMT submillimetre continuum study showed HH24 MMS to have a ratio of total to submillimetre luminosity of < 40, well below the Class 0 upper limit of 200 (Ward-Thompson et al. 1995 – hereafter Paper II). This low $L_{\rm bol}/L_{\rm submm}$ luminosity ratio suggests that the circumstellar envelope mass of HH24 MMS exceeds the mass of the central YSO, hence that the protostar has not yet accumulated the major part of its final main-sequence mass, in contrast to most Class I near-IR YSOs (AWB; André & Montmerle 1994).

The results of Papers I & II together also showed that HH24 MMS has an unusually flat centimetre to millimetre spectral index for thermal dust emission: $\alpha \sim 3$, where $S_\nu \propto \nu^\alpha$. Recent interferometric observations at 3.4 and 7 mm confirmed the flat spectrum, and also suggested the presence of an inner circumstellar disk based on the detection of a compact unresolved source (Chandler et al. 1995). The unresolved disk was estimated to be an order of magnitude less massive than the extended submm clump/envelope (of total mass $M \sim 3 - 6\,{\rm M}_\odot$, cf. Paper II). These findings further rule out the isothermal protostar hypothesis and are consistent with the above interpretation that HH24 MMS harbors a very young Class 0 YSO.

Additional support to this interpretation would be given by the detection of an outflow from HH24 MMS. Indeed, most known Class 0 protostars are observed to drive highly collimated or "jet-like" CO outflows (e.g., André et al. 1990; see Bachiller & Gómez-Gonzalez 1992 for a review). However, the outflow status of HH24 MMS has been a matter for debate. A previous millimetre spectral

line study of the source proved inconclusive, due to the great deal of outflow and jet activity in the HH24 region (Krügel & Chini 1994). In this paper, new deep near-infrared and radio images are presented which, together with CO spectral line data, show that HH24 MMS is indeed the source of a well-collimated jet.

2. Observations and results

2.1. Near-Infrared Observations

Near-IR data were taken with the United Kingdom Infrared Telescope (UKIRT)[1], as part of the UKIRT Service Programme, on the nights of 1994 December $1^{st} - 3^{rd}$. Images were made with the IRCAM3 infrared camera system (Puxley et al. 1994) through two filters, one centred on the 2.122 μm v=1–0 S(1) vibrational transition of H_2, and the other centred on the adjacent continuum at 2.102 μm. The FWHM of both filters is 0.02 μm. The camera is a 256×256 pixel array, which was used with a pixel scale of 0.286 arcsec/pixel. This allowed HH24 MMS and the nearby double near-IR source SSV63E-W to be visible in the same field, helping the registering of the images. The total exposure time on source was 15 min for the S(1) filter and 12 min for the narrow-band continuum image. An adjacent blank field was taken for the off-source position used in the sky subtraction, and the data were flat-fielded in the normal manner.

The data were reduced using the IRCAM software, and calibration was performed using the standard star HD40335, whose K-band magnitude was taken to be 6.452. The narrow-band continuum image was subtracted from the S(1) image, hence the resulting emission is entirely due to the v=1–0 S(1) transition. The mean seeing while the data were taken was estimated from HD40335 to be 1.6″, so the final S(1) image was smoothed with a gaussian filter of FWHM = 5 pixels (1.43″).

Figure 1a and Figure 1b show the final S(1) image (after continuum subtraction) and the continuum image as isophotal contour maps superposed on grey-scales. The position of the VLA source observed in the centre of the submillimetre clump HH24 MMS is marked by a plus sign (see Paper I and Sect. 2.2 below). Figure 1a reveals for the first time a clear jet-like H_2 feature associated with HH24 MMS, extending roughly northeast-southwest. The continuum image (Fig. 1b) shows an unresolved point source of 2.2 μm magnitude $K \sim 15.6$ located $\sim 5''$ away from the VLA source.

[1] UKIRT is operated by the Royal Observatories on behalf of the UK Particle Physics and Astronomy Research Council (PPARC).

Table 2. Flux densities of the radio source VLA #5 associated with HH24 MMS

Component	S_ν (mJy) 6.0 cm	3.6 cm	2.0 cm
Peak	$\lesssim 0.07$	0.13 ± 0.02	0.69 ± 0.08
Integrated	$\lesssim 0.18$	0.33 ± 0.03	0.72 ± 0.1
(Box)	$(45'' \times 45'')$	$(45'' \times 45'')$	$(15'' \times 15'')$
Unresolved	$\lesssim 0.07$	0.11 ± 0.03	0.7 ± 0.1
Extended	$\lesssim 0.18$	0.22 ± 0.06	$\lesssim 0.4$

2.2. Centimeter Continuum Observations

Radio continuum observations of HH24 MMS at 2, 3.6, and 6 cm were obtained with the NRAO[2] Very Large Array (VLA). Session dates, array configurations, and phase centers are listed in Table 1. The 1993 September observations, which were already published in Paper I, are included in Table ?? since they were combined with the new data. For all these observations the total effective bandwidth was 100 MHz and both circular polarizations were observed. The amplitude calibrator was 3C48 for the new data (1995 April and June), and 3C286 for the 1993 sessions. The phase fluctuations were monitored by observing the VLA calibrator 0539-057. The data were edited, calibrated, and imaged using standard routines from the AIPS package. The naturally-weighted beam sizes and rms noises of the 2, 3.6, and 6 cm maps are listed in Table ??.

At 2 cm an unresolved $\sim$ 0.7 mJy source is detected at a position consistent with that of the 3.6 cm source VLA #5 of Paper I which coincides with HH24 MMS. At 3.6 cm, the 1993 and 1995 uv data were combined after checking that the images from the two data sets were consistent in position, flux density, and morphology. A Gaussian fit indicates the 3.6 cm emission from HH24 MMS is resolved with a deconvolved FWHM size of $19.4'' \times 6.7''$ (P.A. 50°). This elongated source, clearly seen in the combined 3.6 cm image shown in Fig. 2, is almost parallel to the near-IR jet (P.A. $\sim$ 40°). At 6 cm, HH24 MMS is not detected to a 5σ upper limit of $\sim$ 70 μJy/beam. Table ?? summarizes the fluxes measured from the VLA maps of Fig. 2.

2.3. CO(3–2) line Observations

Submillimetre spectral line data in the ^{12}CO J=3–2 transition, at 345.796 GHz, were obtained at the James Clerk

[2] The National Radio Astronomy Observatory is operated by Associated Universities, Inc., under cooperative agreement with the National Science Foundation.

Table 1. Journal of the VLA observations

Dates	λ (cm)	Array conf.	Phase center $\alpha(1950)$	$\delta(1950)$	Beam FWHM, P.A.	Map rms (μJy/beam)
1995 April 30	2.0	D	$05^h43^m35^s.1$	$-00°11'47''$	$6.4'' \times 5.3''$, 8.5°	81
1993 Sept. 27, 30	3.6	CnD	$05^h43^m35^s.1$	$-00°11'47''$	$9.2'' \times 8.3''$, 29°	17
& 1995 June 1[a]	3.6	D				
1995 April 30, June 1	6.0	D	$05^h43^m35^s.1$	$-00°12'20''$	$20.2'' \times 16.2''$, 4.4°	14

[a] The 1993 September observations were already published in Paper I. They have been combined with the new data (1995 June).

Maxwell Telescope (JCMT)[3] on Mauna Kea, Hawaii, on 1994 January 1st at U.T. = 06.30–07.30. At this frequency, the FWHM beamsize of the JCMT is $\sim 14''$. The common user receiver RxB3i (Cunningham et al 1992) was used with a digital auto-correlation spectrometer (DAS) backend. Spectra were obtained on a 5×5 grid, with a spacing of 15×15 arcsec. The data were reduced using the SPECX and CLASS packages.

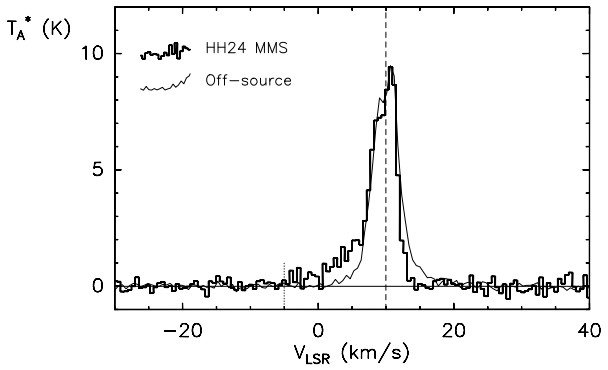

Fig. 3. J=3–2 CO JCMT spectrum taken at the position of HH24 MMS ("on-source" spectrum, histogram line) superposed on an "off-source" spectrum (smooth line) computed by averaging the 8 spectra observed around HH24 MMS. Note the blue-shifted wing at velocities up to -15 km s^{-1} relative to the line centre in the on-source spectrum, and the red-shifted wing in the off-source spectrum.

[3] The JCMT is operated by the Observatories on behalf of the United Kingdom Particle Physics and Astronomy Research Council, the Netherlands Organization for Scientific Research and the Canadian National Research Council.

The data show a profusion of high-velocity molecular gas in this complex region, and it is not possible to precisely identify a bipolar outflow with the HH24 MMS source. This is in agreement with the findings of Krügel & Chini (1994). However, in Fig. 3 we show the spectrum taken at the central position of HH24 MMS itself, together with a mean "off-source" spectrum taken at a mean projected distance of $\sim 20''$ from HH24 MMS. It can be seen that the "on-source" spectrum has a blue wing at velocities up to ~ -15 km s^{-1} from line centre which is not present in the mean off-source spectrum. We here suggest that this blue-shifted emission is the molecular manifestation of the jet-like feature seen in our H_2 S(1) and radio continuum data. Note that the observed maximum CO velocity is relatively high and that, according to the criteria used by Bontemps et al. (1996) in their recent homogeneous survey for CO outflows around low-mass YSOs, HH24 MMS would be classified as a molecular outflow source. One can also clearly see a red-shifted wing in the off-source spectrum of Fig. 3. Some of this emission is probably related to the SSV63 jets which are red-shifted in the HH24A region.

By integrating the CO(3–2) emission associated with HH24 MMS over the blue-shifted wing from -5 to 7 km s^{-1}, we estimate that the mass and momentum contained in the high-velocity molecular gas are $M_{\rm CO} \sim 10^{-3}\,{\rm M}_\odot$ and $P_{\rm CO} \sim 7 \times 10^{-3}\,{\rm M}_\odot\,{\rm km\,s}^{-1}$ respectively, without any correction for inclination or line opacity at low velocity. Because of confusion from the SSV63 jets and the compactness of the HH 24MMS outflow, it is difficult to apply the systematic procedure of Bontemps et al. (1996) in order to derive a momentum flux $\dot{P}_{\rm CO}$ from our CO(3–2) map. Assuming all the "off-source" high-velocity gas is associated with HH 24MMS (while some is likely associated with the SSV63 jets), we obtain an upper

limit to $\dot{P}_{\rm CO}$ of $\lesssim 9\times10^{-5}\,{\rm M}_\odot\,{\rm km\,s^{-1}yr^{-1}}$ after correction for inclination and opacity effects[4].

3. An H_2 IR jet emanating from HH24 MMS

The shocked H_2 S(1) emission detected near HH24 MMS shows a clear jet morphology and consists of at least four knots labelled NE 1 & 2 and SW 1 & 2 in Fig. 1. The main jet feature (knots NE 1 and SW 1) is seen in projection towards the submm dust clump (see Fig. 4). It has an apparent length $\lesssim 10''$ corresponding to $\lesssim 0.02$ pc, and is virtually unresolved in its transverse direction with a width $\sim 2-2.5\,''$ in the unsmoothed image. The knot NE 2 coincides with the southernmost part of the optical HH object HH24A[5] which has been associated with the SSV63E jet in the literature (e.g., Jones et al. 1987; Mundt, Ray, & Raga 1991). On the basis of its northeast-southwest elongated morphology (see Fig. 1a), we here argue that the NE 2 feature is in fact associated with the main HH24 MMS jet. In this respect, it is noteworthy that the optical knot called HH24As′ by Jones et al. (1987, see their Table IV) coincides with NE 2 and is *blueshifted* ($v_{\rm rad} = -38\,{\rm km\,s^{-1}}$). This contrasts with the jet from SSV63E which is *redshifted* on that side of the source (see knot E of Jones et al. 1987). HH24As′ is also the highest-density HH optical knot of the area with $n_e \sim 10^4$ cm^{-3}. The H_2 knot SW 2 is the faintest of all the knots we detect at 2 μm. It is located nearly symmetrically of the NE 2 knot with respect to the central jet feature.

The good spatial coincidence between the central H_2 jet and the submm clump HH24 MMS mapped in Chini et al. (1993) & Paper II strongly suggests the two are physically associated (see Fig. 4). However, the detailed structure on scales less than $\sim$ 10 arcsec (0.02 pc) is unknown, due to the limited resolution of the millimetre and submillimetre data. In addition, the positions of the H_2 knots with respect to the VLA source features are uncertain. The relative astrometry of the UKIRT and VLA images introduces a total alignment uncertainty of ≤ 5 arcsec (see below).

If we assume that the 2.2 μm (continuum) counterparts of SSV63W and SSV63E coincide exactly in position with the compact VLA sources VLA #3 and VLA #6 of Fig. 2 and Paper I, then we obtain the relative positioning shown in Fig. 1, where the center of HH24 MMS, taken to be that of VLA #5, is marked by a cross. However, the 2.2 μm sources have a diffuse morphology and may be reflection nebulosities displaced from the actual YSOs SSV63W and SSV63E (see also Moneti and Reipurth 1995). Such offsets are frequent among embedded IR jet sources and may amount to several arcseconds along the jet axes (see the example of HH 111 in Stapelfeldt & Scoville 1993). For this reason, we believe that our registering of the VLA and IR images is not good to better than $\sim 5''$ in the direction of the jets from SSV63W and SSV63E and $\sim 2''$ perpendicular to these jets. We have drawn a corresponding error ellipse around the cross in Fig. 1. When considered together with the jet-like morphology of the H_2 emission, the error ellipse of Fig. 1 suggests that the center of HH24 MMS is located on the jet axis somewhere between NE1 and SW1. In this view, the weak 2.1 μm continuum point source seen in Fig. 1b (which apparently coincides with the H_2 knot NE 1) would be a very compact (hence young) reflection nebula in the blue-shifted part of the jet. (This would be consistent with the blue-shifted nature of the optical knot HH24As′, see above).

Fig. 4. Overlay of the UKIRT H_2 S(1) image of Fig. 1a (grey-scale), the 3.6 cm VLA image of Fig. 2a (solid contours), and the IRAM 1.3 mm dust continuum image of Chini et al. (1993) (dotted contours).

Figure 4 displays the relative positioning proposed above in the form of an overlay of the 1.3 mm continuum map from Chini et al. 1993, our H_2 image of the jet, and our VLA image of the 3.6 cm continuum emission. Fig. 4 shows that the central H_2 jet NE1-SW1 is probably entirely embedded within the HH24 MMS protostellar clump while the two secondary H_2 components NE2 and SW2 lie on either side of the clump. This suggests that the central H_2 knots NE1 and SW1 suffer a much higher extinction than the secondary components NE2 and SW2. In Paper II, the submm continuum emission from HH24 MMS was fitted by an elliptical Gaussian source, unresolved along its minor axis (FWHM $< 18''$), and of deconvolved FWHM size $\sim 21''$ along its major axis (P.A. $\sim 124°$). Assuming a dust temperature of 20 K,

[4] We use the same mean correction factor for inclination and opacity as Bontemps et al. (1996).

[5] HH24A was also detected in the H_2 S(1) line by Zealey et al. (1989) (see also Lane 1989).

the total mass under the Gaussian was estimated to be $M_{\rm tot} \approx 3-6\,{\rm M}_\odot$ depending on the uncertain dust opacity (see Henning et al. 1995 and references therein), yielding a mean column density $N_{\rm H_2} \approx 1-2\times10^{23}$ cm^{-2} and a mean density $n_{\rm H_2} \gtrsim 3-6\times10^{6}$ cm^{-3}. (Recall that only a small, $\leq 10\%$ fraction of the total mass is contained in a compact disk – Chandler et al. 1995.) For an ellipsoidal source, this corresponds to a (one-sided) mean extinction $A_{\rm K} \approx 5-10$ at 2.2 μm.

In turn, such high values of $A_{\rm K}$ would imply a high intrinsic H_2 luminosity and surface brightness for the jet. Assuming the luminosity radiated in all shocked H_2 lines is a factor of 10 that of the v=1–0 S(1) line (which is the case for 2000 K hydrogen – Scoville 1982), the total H_2 luminosity $L_{\rm H_2}$ from the HH24 MMS jet is related to the integrated H_2 S(1) flux $F_{\rm S(1)} = 3.5\times10^{-14}$ erg cm^{-2} s^{-1} observed in the two primary knots NE1 and SW1 by: $L_{\rm H_2} = 10^{\frac{A_{\rm K}}{2.5}} \times 10 \times 4\,\pi\,{\rm d}^2 \times F_{\rm S(1)}$. (Since the extinction is probably much lower toward the two secondary knots NE2 and SW2, the intrinsic H_2 luminosity of the jet is dominated by that of the primary knots.) Similarly, since the emitting surface of the jet is $S_{\rm em} \lesssim 10\times2$ arcsec^2 $\sim 4.7\times10^{-10}$ sr, its intrinsic surface brightness must be $I_{\rm S(1)} \gtrsim 7.5\times10^{-5}\times10^{\frac{A_{\rm K}}{2.5}}$ erg cm^{-2} s^{-1} sr^{-1}. We obtain $L_{\rm H_2} \approx 23$ L$_\odot$ and $I_{\rm S(1)} \gtrsim 0.75$ erg cm^{-2} s^{-1} sr^{-1} if the mean extinction is $A_{\rm K}=10$, but only $L_{\rm H_2} \approx 0.23$ L$_\odot$ and $I_{\rm S(1)} \gtrsim 7.5\times10^{-3}$ erg cm^{-2} s^{-1} sr^{-1} if $A_{\rm K}=5$. The higher value of $L_{\rm H_2}$ can probably be ruled out since it is $\gtrsim 4$ times larger than the total bolometric luminosity of HH24 MMS ($L_{\rm bol} \approx 5.3$ L$_\odot$, see Paper II). The lower values of $L_{\rm H_2}$ and $I_{\rm S(1)}$ would still be remarkably high but not untypical of these kinds of (Class 0) sources (see Davis & Eislöffel 1995 and Sect. 5 below).

4. Radio emission from the jet

The centimeter radio continuum emission detected around HH24 MMS may be divided into a central unresolved component detected at both 3.6 and 2 cm, and an elongated jet-like component detected only at 3.6 cm (see Fig. 2 and Table ??). The unresolved component is most likely the cm counterpart of the compact dust disk identified by Chandler et al. (1995) at 3.4 and 7 mm. The spectral index we estimate for this component between 3.6 and 2 cm is high ($\alpha \approx 3$) and consistent with the spectrum of the dust disk between 7 and 3.4 mm (Chandler et al. 1995).

On the other hand, the elongated 3.6 cm component cannot arise from dust since the extended submm dust envelope/clump is unlikely to contribute significant continuum emission at this wavelength (see Fig. 3 of Chandler et al. 1995). Furthermore, the jet-like morphology of this component (Fig. 2) is very reminiscent of the H_2 IR jet seen in Fig. 1. This is illustrated further in Figure 4 where we have overlaid the radio map (displayed as solid contours) on a grey-scale version of the IR S(1) image, assuming that VLA #5 lies in between the H_2 knots NE1 and SW1 (see Sect. 3 above). Thus, we propose that the elongated radio component arises from free-free emission in the shock-ionized fraction of the jet, as frequently observed in outflow sources (e.g., Anglada 1995). Based on the integrated emission we measure at 3.6 cm, we estimate that the total flux of the radio jet is $S_{3.6cm} \sim 0.2$ mJy (see Table ??). This flux is consistent with our non-detection of HH24 MMS at 6 cm, assuming a typical spectral index $\alpha \gtrsim 0$ for the ionized jet (corresponding to mostly optically thin free-free emission; e.g., Reynolds 1986; Rodríguez 1995).

Following this interpretation, the observed flux density $S_{3.6cm}$ of the jet may be used to derive a crude, indirect estimate of the outflow momentum rate $\dot{P}$. The centimeter radio luminosity is indeed expected to be proportional to $\dot{P}$ in the shock-ionized scenario of Curiel, Cantó, & Rodríguez (1987). This correlation was confirmed observationally by Anglada (1995) for a sample of 29 outflow sources. Assuming that HH24 MMS falls on the Anglada correlation, we infer $\dot{P} \sim 10^{-4}\,{\rm M}_\odot\,{\rm km\,s^{-1}yr^{-1}}$. Such a value of $\dot{P}$ would imply $\dot{P}c/L_{\rm bol} \approx 1000$ which is quite typical for Class 0 sources (see Bontemps et al. 1996).

One also verifies that the minimum mechanical luminosity required to shock-ionize the radio jet remains in a plausible range. Assuming optically thin free-free emission, the observed 3.6 cm flux density implies a volume emission measure ${\rm EM_V} = 1.2\times10^{55}$ cm^{-5}. If the standard case B recombination theory holds, then the minimum luminosity needed to keep the jet ionized is $L_{\rm ion} = \alpha^{(2)}(T)\,{\rm EM_V}\,{\rm E_{ion}} \approx 0.02\,{\rm L}_\odot$ where ${\rm E_{ion}} = 13.6$ eV (e.g., Spitzer 1968).

5. Implications for the jet structure

The jet from HH24 MMS is unusual in that it is remarkably short with a total projected length of $\lesssim 0.07$ pc. Furthermore, the main interaction between the jet and the surrounding material apparently occurs very close to the central source, at a projected distance $\lesssim 0.01$ pc, which is of the order of the circumstellar clump size. By comparison, the young outflow source L1448-C shows strong interactions with ambient material at much larger distances ($\sim 0.05-0.1$ pc; e.g., Bally, Lada, & Lane 1993). The same is true for the other young Class 0 protostars with known IR H_2 jets (e.g., VLA1623 and L1157; see Davis & Eislöffel 1995).

We suggest that the remarkable properties of the HH24 MMS jet indicate that mass ejection turned on only very recently in this protostellar system. The short length and youth of the HH24 MMS jet may account for the absence of a well-developed CO outflow in this source. Indeed, a very young jet would not have had time to entrain much molecular material and its associated outflow would itself be extremely compact.

Another remarkable feature of the HH24 MMS jet is that it exhibits both H_2 emission and radio continuum emission at the same location. In most embedded outflow sources the dense inner jet is similarly observed at centimeter wavelengths (e.g., Rodríguez 1995; Anglada 1995), but IR H_2 emission is detected only at large distances from the central YSO. This difference may result from peculiar excitation conditions in the jet.

The high intrinsic H_2 luminosity suggested in Sect. 3 for the central HH24 MMS jet would be indicative of a nondissociative C-type shock of velocity $v_{\rm sh} \lesssim 40\,{\rm km\,s^{-1}}$. More than 99 % of the total power dissipated in the shock then emerges in molecular lines (e.g., Draine et al. 1983; Neufeld & Dalgarno 1989). On the other hand, only fast ($v_{\rm sh} \gtrsim 40\,{\rm km\,s^{-1}}$), dissociative J-type shocks can generate enough ionization to produce detectable free-free radio continuum emission (see McKee & Hollenbach 1987 and Curiel et al. 1987). (The degree of ionization is maintained at low levels $n_e/n \lesssim 10^{-4}$ in C shocks.) These apparently contradictory requirements implied by the simultaneous detection of H_2 and radio continuum emission may be reconciled if the jet has a bow shock structure (e.g., Raga et al. 1990; Davis, Mundt, & Eislöffel 1994). In this case, the H_2 emission could arise from the bow shock wings (where the shocks are oblique and have relatively low velocities, see Smith 1994), while the radio emission would derive from the working surface itself (where the shocks are nearly parallel and have higher velocities).

6. Conclusions

The near-IR and radio continuum observations presented in this paper clearly establish that a collimated jet is emanating from the protostellar clump HH24 MMS.

The detected near-IR H_2 emission consists of a main central jet, deeply embedded within the protostellar clump and likely suffering a large extinction ($A_{\rm K} \gtrsim 5$), and of two H_2 knots which lie at the edges of the high density, highly obscured region of the HH24 MMS clump. The intrinsic H_2 luminosity, dominated by the main central jet, is $\sim 0.23\,{\rm L}_\odot$ assuming a mean extinction $A_{\rm K} = 5$. However, the actual extinction and luminosity are poorly known due to the unknown matter distribution on small scales and the uncertain dust emissivity at millimeter wavelengths.

The HH24 MMS jet is likely a very young jet, still mainly interacting with the central protostellar clump and without any large scale manifestations such as a well-developed CO outflow.

These findings confirm the conclusion of Paper I and Paper II that the dense clump HH24 MMS has passed the isothermal phase of protostellar collapse and contains a (hydrostatic) Class 0 protostar. Indeed, we now know that HH24 MMS possesses all three usual observational attributes of Class 0 YSOs (cf. AWB): high ratio of submillimetric to bolometric luminosity (Chini et al. 1993 and Paper II), compact centimetre radio continuum emission (Paper I), and presence of a collimated jet (this paper). This suggests that, once rapid protostellar collapse sets in, a cloud core remains isothermal only for a time shorter than the Class 0 phase (whose estimated timescale $t \sim 10^4$ yr).

Our results also strongly suggest that jet-like outflows are a common feature of *all* Class 0 objects. Most Class 0 sources were actually identified by means of their collimated CO outflows (see Barsony 1994 and André 1995 for recent reviews), but a few of them were initially discovered through their strong submillimetre dust emission (e.g., HH24 MMS; Chini et al. 1993) or their VLA radio continuum emission (e.g., VLA 1623; Leous et al. 1991). The example of HH24 MMS illustrates that, no matter how a Class 0 protostar is discovered, one always ends up finding a jet around it. This reinforces the view according to which the outflow phase coincides with the accretion phase, and starts as soon as a hydrostatic core forms at the center of a collapsing cloud.

Acknowledgements. We are grateful to Colin Aspin for taking the near-IR data for us as part of the UKIRT Service Programme. We would also like to thank the British Council and the French APAPE for financial assistance for travel in the form of Alliance grant number PN95.219.

References

André P. 1995, in "Circumstellar Matter", Ed. G.D. Watt & P.M. Williams, Ap&SS, 224, 29
André P., Montmerle T. 1994, ApJ, 420, 837
André P., Martín-Pintado J., Despois D., Montmerle T. 1990, A&A, 236, 180
André P., Ward-Thompson D., Barsony M. 1993, ApJ, 406, 122 (AWB)
Anglada G. 1995, in "Circumstellar disks, outflows and star formation", RevMexAA (Serie de Conf.), 1, 67
Bachiller R., Gómez-González J. 1992, A&AR, 3, 257
Bally J., Lada E.A., Lane A.P. 1993, ApJ, 418, 322
Barsony M. 1994, in "Clouds, Cores, and Low-mass Stars", Ed. D.P. Clemens & R. Barvainis, A.S.P. Conf. Series, 65, 197
Bontemps S., André P., Ward-Thompson D. 1995, A&A, 297, 98 (Paper I)
Bontemps S., André P., Terebey S., Cabrit S. 1996, A&A, in press
Chandler C.J., Koerner D.W., Sargent A.I., Wood D.O.S. 1995, ApJ, 449, L139
Chini R., Krügel E., Haslam C.G.T., Kreysa E., Lemke R., Reipurth B., Sievers A., Ward-Thompson D. 1993, A&A, 272, L5
Cunningham C. T., et al 1992, Int. J. Infrared and Millimeter Waves, 13, 1827
Curiel S., Cantó J., Rodríguez L.F. 1987, RevMexAA, 14, 595
Davis C.J., Mundt R., Eislöffel J. 1994, ApJ, 437, L55
Davis C.J., Eislöffel J. 1995, A&A, 300, 851
Draine B.T., Roberge W.G., Dalgarno A. 1983, ApJ, 264, 485
Henning T., Michel B., Stognienko R. 1995, Planet. Space Sci., Vol.43, 10/11, 1333
Jones B.F., Cohen M., Wehinger P.A., Gehren T. 1987, AJ, 94, 1260

Krügel E., Chini R. 1994, A&A, 287, 947
Lane A.P. 1989, in ESO Workshop on "Low Mass Star Formation and Pre-Main Sequence Objects", Ed. B.Reipurth, p. 331
Leous J.A., Feigelson E.D., André P., Montmerle T. 1991, ApJ, 379, 683
McKee C.F., Hollenbach D.J. 1987, ApJ, 322, 275
Mundt R., Ray T.P., Raga A.C. 1991, A&A, 252, 740
Neufeld D.A., Dalgarno A. 1987, ApJ, 344, 251
Puxley P.J., Sylvester J., Pickup D.A., Paterson M.J., Laird D.C., Atad-Ettedgui E.I. 1994, In "Instrumentation in Astronomy VIII", Ed. D.L. Crawford, E.R. Craine, SPIE, Washington, Vol. 2198, 350
Raga A.C., Binette L., Cantó J. 1990, ApJ, 360, 612
Reynolds S.P. 1986, ApJ, 304, 713
Rodríguez L.F. 1995, in "Circumstellar disks, outflows and star formation", RevMexAA (Serie de Conf.), 1, 1
Scoville N.Z., Hall D.N.B., Kleinmann S.G., Ridgeway S.T. 1982, ApJ, 253, 136
Smith M.D. 1994, MNRAS, 266, 238
Stapelfeldt K.R., Scoville N.Z. 1993, ApJ, 408, 239
Strom K. M., Strom S. E., Vrba F. J., 1976, AJ, 81, 308
Ward-Thompson D., Chini R., Krügel E., André P., Bontemps S., 1995, MNRAS, 274, 1219 (Paper II)
Zealey W.J., Mundt R., Ray T.P., Sandell G., Geballe T., Taylor K.N.R., Williams P.M., Zinnecker H. 1989, Proc.Astr.Soc.Austr., 8, 62

This article was processed by the author using Springer-Verlag LaTeX A&A style file *L-AA* version 3.

Figure captions

Fig. **1.** Isophotal contour maps superposed on grey-scale of (a) the 2.122 μm $v=1-0$ S(1) H_2 emission detected near HH24MMS (after continuum subtraction), and (b) the adjacent, continuum emission at 2.102 μm. In both maps, the contour levels are 1.5, 3, 5, 8, 15, 30 x 10^{16} erg cm^{-2}s^{-1}arcsec^{-2}. The position of the 2-cm VLA source detected at the centre of HH24 M MS is marked by a plus surrounded by an error ellipse (see text). The jet-like S(1) feature consists of four knots labelled NE 1 & 2 and SW 1 & 2. The axes of the jets from SSV63 are shown as dashed lines. The H H object HH24A is probably associated with the jet driven by SSV63E.

Fig. 2. VLA images of the radio continuum emission from HH24MMS.
(a) 3.6 cm image from the 1993 Sept. /1995 June combined data. The contour levels are –2, 2, 3.2, 5, 8, 12.5 times the rms noise (17 μJy/beam). The VLA sources labelled # 3, # 5 and # 6 refer to the sources of Paper I and are identified as SSV63W, SSV63E and HH24MMS respectively.
(b) 2 cm image from the 1995 April 30 data. The contour levels are –3, 3, 4, 5.3, 7.1 times the rms noise (81 @y/beam).

Fig. **3.** J=3–2 CO JCMT spectrum taken at the position of HH24MMS ("on-source" spectrum, histogram line) superposed on an "off-source" spectrum (smooth line) computed by averaging the 8 spectra observed around HH24MMS. Note the blue-shifted wing at velocities up to —15 km s^{-1} relative to the line centre in the on-source spectrum, and the red-shifted wing in the off-source spectrum.

Fig. 4. Overlay of the UKIRT H_2 S(1) image of Fig. la (grey-scale), the 3.6 cm VLA image of Fig. 2a (solid contours), and the IRAM 1.3 mm dust continuum image of Chini et al. (1993) (dotted contours).

This article was processed by the author using Springer-Verlag LaTeX A&A style file 1990.

Figure 1 a-b

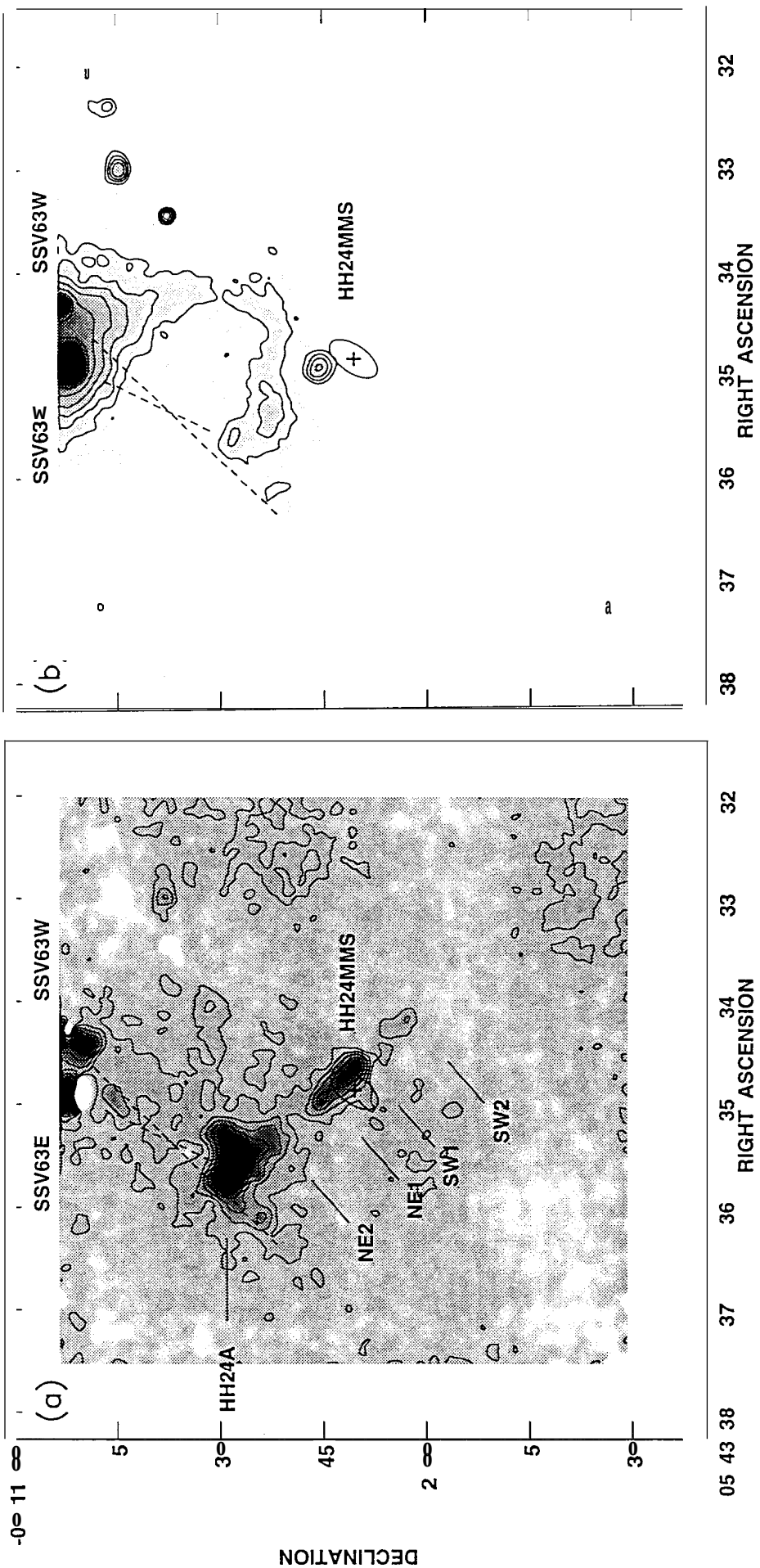
(a)
SSV63E
SSV63W
HH24MMS
HH24A
NE2
NE1
SW1
SW2
(b)
SSV63E
SSV63W
HH24MMS
RIGHT ASCENSION
DECLINATION

Figure 2 a-b

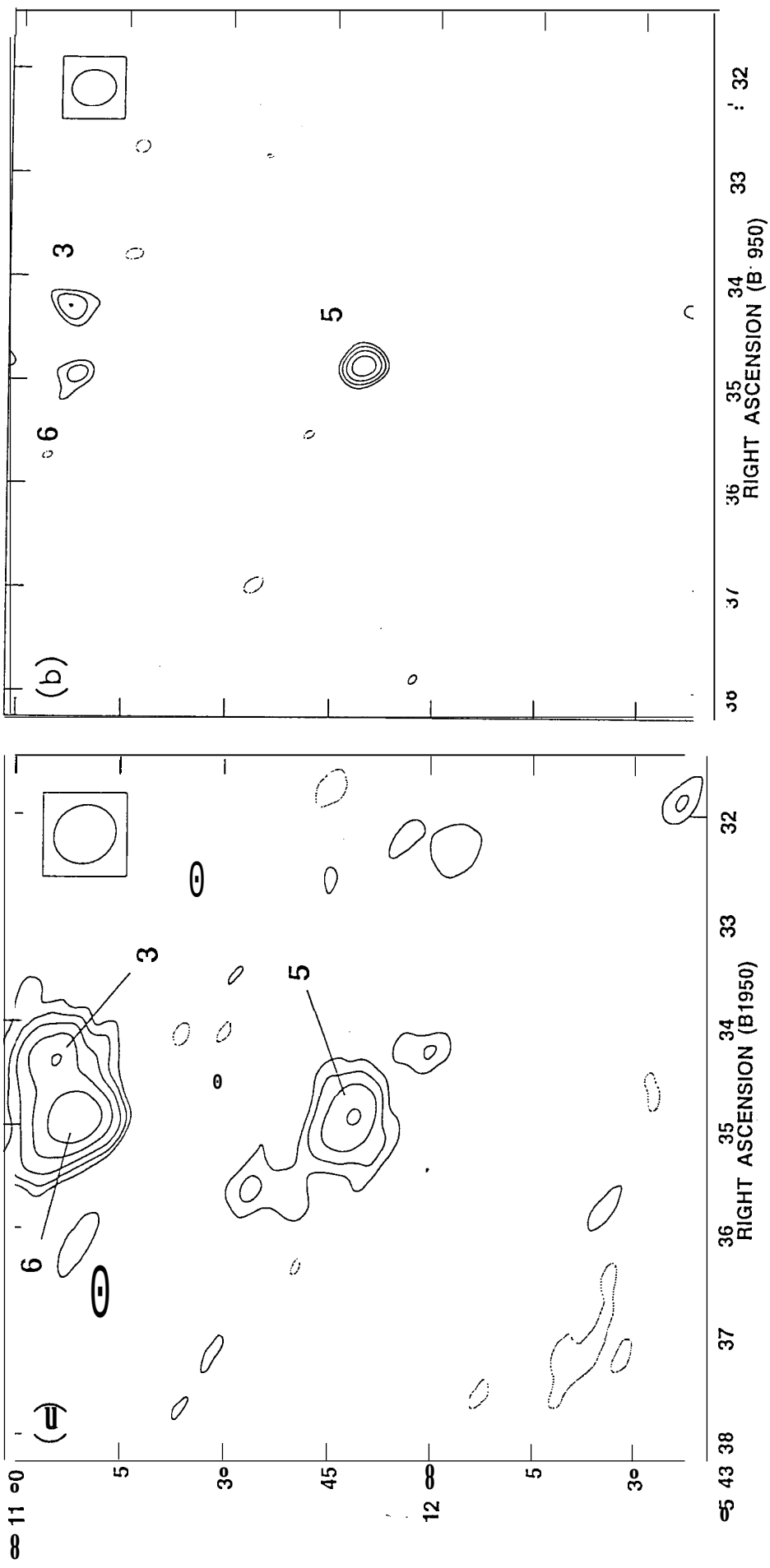
(b)
3
5
6
RIGHT ASCENSION (B 950)
(a)
3
5
6
RIGHT ASCENSION (B1950)
DECLINATION (B1950)

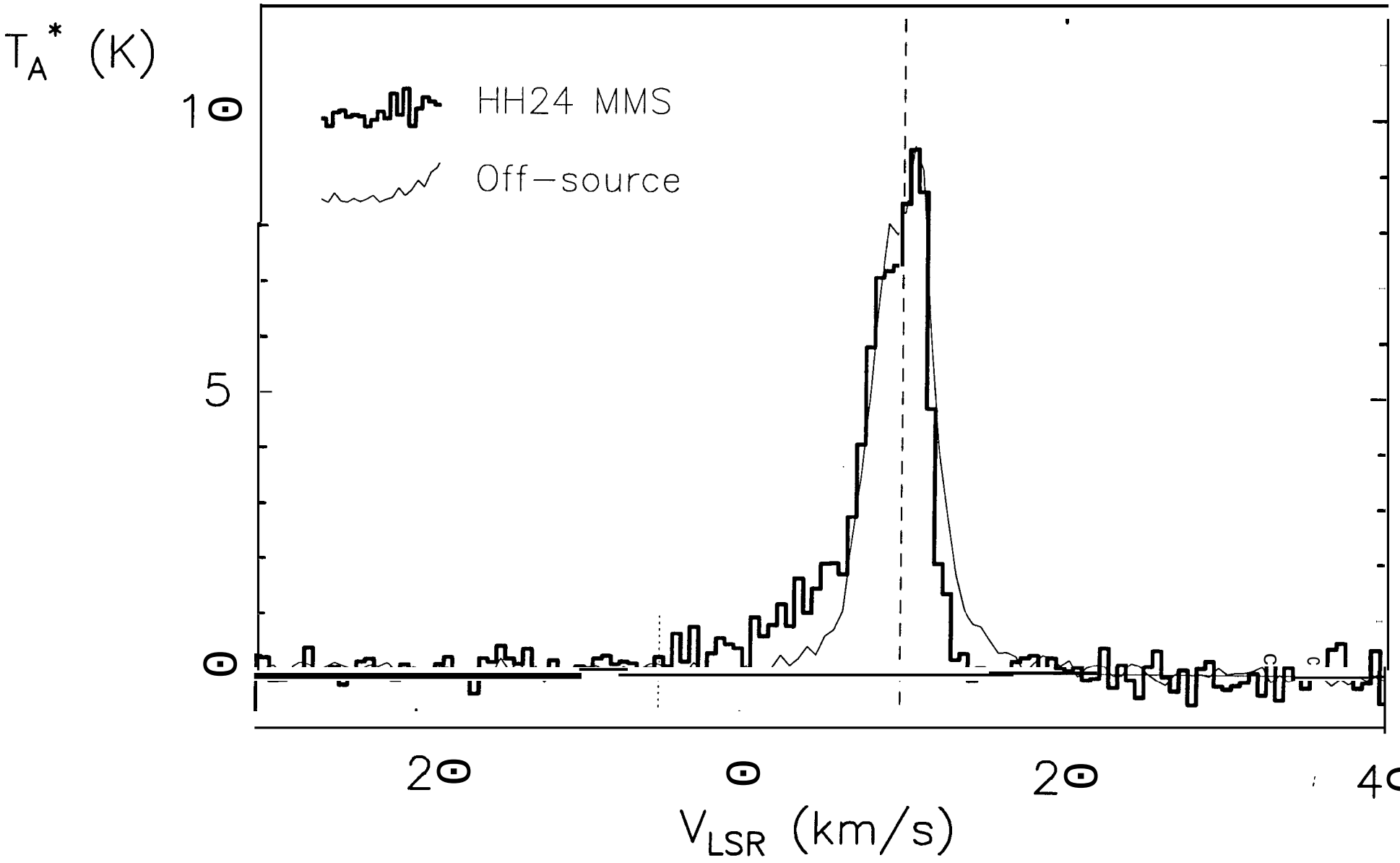

Figure 3

Figure 4

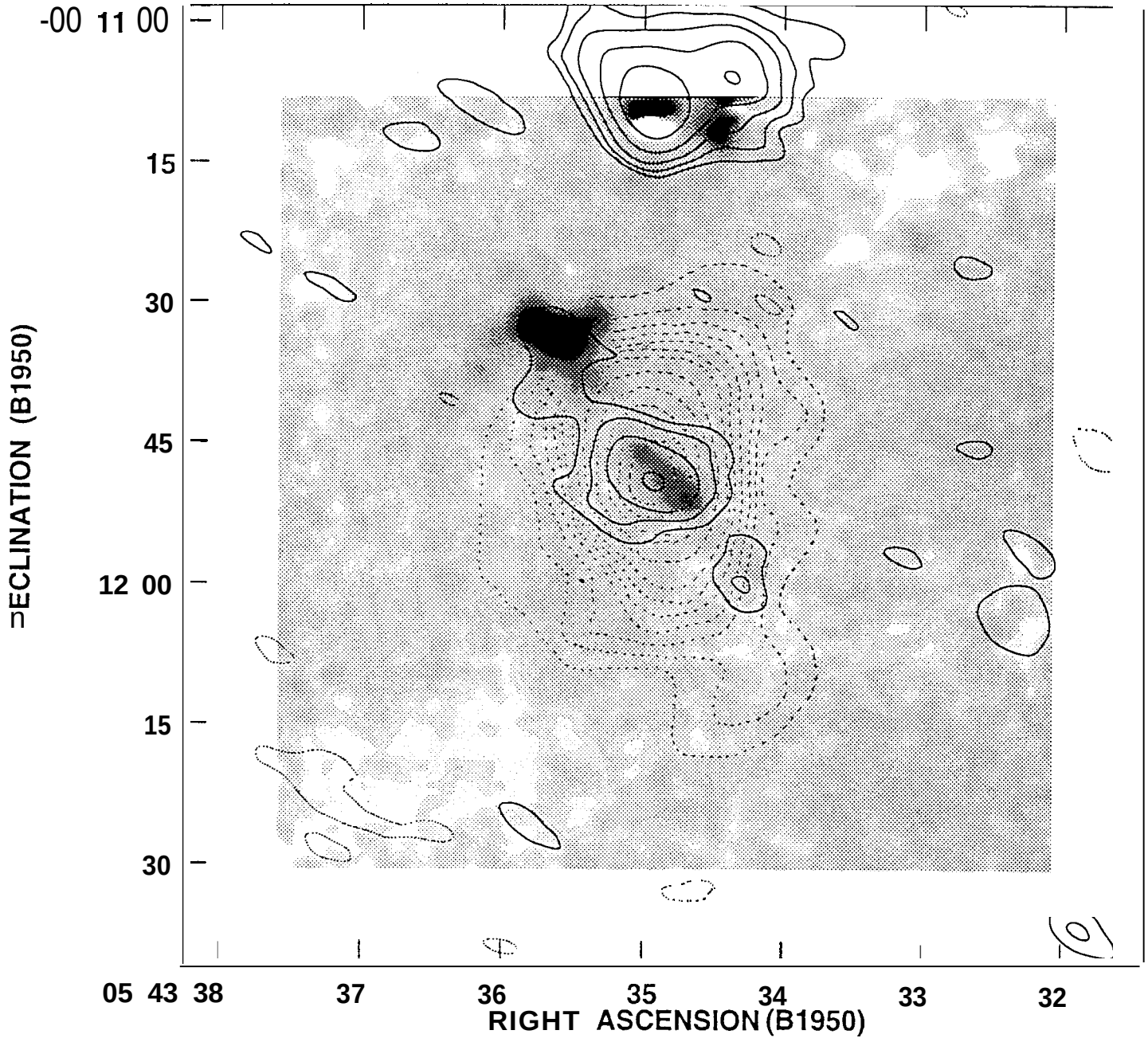
-00 11 00
15
30
45
12 00
15
30
DECLINATION (B1950)
05 43 38
37
36
35
34
33
32
RIGHT ASCENSION (B1950)